# Image Segmentation and Transfer Learning Approach for Skin Classification

Hiep Xuan Huynh[1(✉)], Cang Anh Phan[2], Loan Thanh Thi Truong[3], and Hai Thanh Nguyen[1]

[1] College of Information and Communication Technology, Can Tho University, Can Tho 900000, Vietnam
{hxhiep, nthai.cit}@ctu.edu.vn
[2] Faculty of Information Technology, Vinh Long University of Technology Education, Vinh Long, Vietnam
cangpa@vlute.edu.vn
[3] Cai Nhum Town High School, Vinh Long, Vietnam

**Abstract.** Skin problems are not only detrimental to physical health but also cause psychological. Especially for patients with damaged or even disfigured faces. In recent years, the incidence of skin diseases has increased rapidly. The medical examination of skin lesions is not a simple task. There are similarities among skin lesions where the doctor's experience with a little inattention can give an inaccurate diagnosis. The automatic classification of skin lesions is expected to save effort, time, and human life. This work has deployed a method using the pre-trained MobileNet model on about 1,280,000 images from the 2014 ImageNet challenge and refined over 25,331 images of the International Skin Imaging Collaboration (ISIC) 2019 dataset. Transfer learning was applied, replacing the classifier with an active softmax layer with three or eight types of skin lesions. An accuracy measure is used to evaluate the performance of the proposed method.

**Keywords:** Skin lesions · Segmentation · Classification · Transfer learning

## 1 Introduction

Screening and early diagnosing are decisive issues to the effectiveness of treatment for patients, especially cancer. Modern medicine has researched and applied many methods to help early diagnosis with high accuracy, in which diagnostic imaging plays an important role. If the test serves as an indirect "sighting" of the disease, abnormalities can be detected through blood and urine tests (sometimes with a check of stool and other secretions), and then diagnostic imaging is to see


P. Cong Vinh and A. Rakib (Eds.): ICCASA 2021, LNICST 409, pp. 179–191, 2021.
https://doi.org/10.1007/978-3-030-93179-7_14

the injury "directly", even while still a source of danger. However, understanding and applying imaging techniques for screening are not easy. Doctors will depend on age, sex, personal history, and family history to screen and precisely diagnose the disease. Image classification is essential in the medical to determine the class labels of test images based on knowledge gathered from training data. The authors [1] propose a new Large Local Margin Estimate classification model with a sparse representation based on a subcategory. The authors [2] propose a new prediction model that classifies skin lesions into benign or malignant lesions using Convolutional Neural Network with Novel Regularizer. The authors [3] propose a fully automatic calculation method for skin lesion classification using optimized depth features from many well-established CNNs and some abstraction levels. However, medical imaging presents not only large differences but also similarities among classes in object space. This affects the accuracy of the classification.

Some skin lesions resemble melanoma. Tumors develop when cells reproduce too quickly. It can be seen or felt, in other cases, it will only be detected on imaging tests. However, using human vision to detect melanoma in images can be inaccurate as it depends on the physician's experience. In lesion detection, image classification is the ultimate goal of medical image analysis to differentiate among diseases. One of the main challenges of image classification is the large differences among classes. Establishing the medical image classification model is a big step forward in the field of disease diagnosis.

In this paper, we propose a new approach with transfer learning [4] for skin lesions classification. Use weights and features of the pre-trained MobileNet model [5] in the ImageNet dataset [6]. According to the previous research, MobileNet is a good extraction feature for imaging classification, object detection, and segmentation. The contributions of the proposed system can be summarized as follows: Image segmentation based on the Superpixels method to divide normal skin and skin lesions and Skin classification with transfer learning.

The remainder of this work is presented as follows. Section 2 introduces the details about the skin lesions. Section 3 introduces the proposed method for skin classification with Transfer learning. Section 4 presents processing. We give a short description of the dataset, tools, and experiment results in Sect. 5. Finally, we conclude in Sect. 6.

## 2 Skin Lesions

Skin lesions [7] is a part of the skin that has unusual growth or appearance relative to the skin around it. There are two types of skin lesions, primary and secondary. Primary skin lesions are abnormal skin conditions present at birth, with skin color changes called macules, which are flat lesions on the skin surface, neither raised nor infiltrated. A liquid lesion is a bulging sack of the epidermis, which contains fluid: vesicles, pustules, or firm lesions: papules, nodules, warts, keratosis. Secondary skin lesions are lesions that have been deformed during the pathological process, as a result of the disease or as a result of treatment.

Secondary skin lesions include scale, crust, excoriation, erosion, fissure, ulcer, atrophy, skin spots, scarring, fibrosis, lichenification.

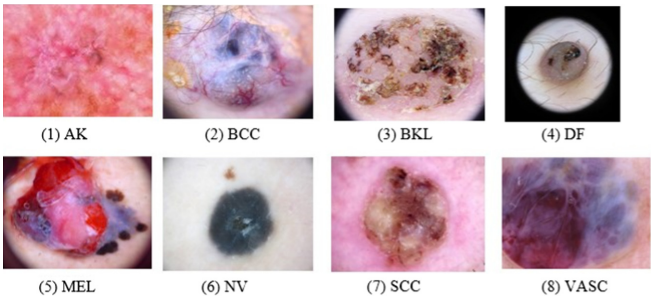


**Fig. 1.** One sample of each class from the ISIC 2019.

Skin lesions come in many different shapes such as linear lesions with the shape of a straight line, annular lesions, nummular lesions with a circular or coin shape, and target lesions (bull's eye or iris) appearing as rings with central opacity, Serpiginous lesions with linear, branching, and curvilinear elements, reticular lesions with a thread or lattice pattern, Verrucous lesions with irregular surfaces, stones, or rough, ... The basic types of skin lesions (Fig. 1 - One sample of each class from the ISIC 2019): Actinic Keratosis [8,9], Basal cell carcinoma [10], Benign keratosis [11–13], Dermatofibroma [14], Melanoma [15,16], Melanocytic nevus [17], Squamous cell carcinoma[1] and The vascular lesion [18,19]. The basic types of skin lesions are shown in Table 1.

## 3 Skin Lesions Classification with Transfer Learning

### 3.1 Segmentation with Superpixels

Segmentation is the identity of specific pixels that make up the object of interest. For example, Superpixels [20] are introduced by Ren and Malik [21] in 2003, superpixels group the same pixels in color and other low-level attributes. In this regard, superpixels solve two problems inherent to digital image processing. First, pixels are merely the result of arbitrariness. Second, the high number of pixels in a large image causes many algorithms that are not computationally feasible. Therefore, Ren and Malik introduced superpixels as more natural entities - grouping pixels that belong to each other while significantly reducing the number of primitives for subsequent algorithms.

A superpixel can be defined as a group of pixels with common characteristics (such as pixel intensity). Superpixel is becoming useful in image processing algorithms and computer vision, such as image segmentation, semantic labeling, object detection, and tracking.

[1] https://www.skincancer.org/skin-cancer-information/squamous-cell-carcinoma/.

**Table 1.** The basic types of skin lesions.

| Skin lesions | Cause | Characteristics |
|---|---|---|
| Actinic Keratosis | - It is considered precancerous or an early form of cutaneous<br>- A scaly spot found on sun-damaged skin | - A flat or thickened papule or plaque-White or yellow; scaly, warty or horny surface<br>- Skin coloured, red or pigmented<br>- Tender or asymptomatic<br>- 1cm to 2cm in size |
| Benign keratosis | A harmless warty spot that appears during adult life as a common sign of skin ageing | - Flat or raised papule or plaque<br>- Skin coloured, yellow, grey, light brown, dark brown, ...<br>- Smooth, waxy or warty surface<br>- 1 mm to several cm in diameter |
| Basal cell carcinoma | - Common form of skin cancer<br>- DNA mutations in the patched (PTCH) tumour suppressor gene<br>- exposure to ultraviolet radiation | - Slowly growing plaque or nodule<br>- Skin coloured, pink or pigmented<br>- Spontaneous bleeding or ulceration<br>- a few mm to several cm in diameter |
| Squamous cell carcinoma | - A common type of keratinocytecancer or non-melanoma skin cancer<br>- Associated with numerous DNA mutations in multiple somatic genes | - Grow over weeks to months<br>- May ulcerate<br>- Tender or painful<br>- Located on sun-exposed sites<br>- a few mm to several cm in diameter |
| Melanoma | - A potentially serious type of skin cancer<br>- An uncontrolled proliferation of melanocytic stem cells that have undergone a genetic transformation | - An unusual looking freckle or mole<br>- A variety of colours: tan, dark brown, black, blue, ...<br>- Itchy or tender, bleed easily or crust over<br>- a few mm-cm in diameter |
| Dermatofibroma | - A common benign fibrous nodule usually found on the<br>- Minor trauma including insect bites, injections, or a rose thorn injury | - Occur anywhere on the skin<br>- Skin dimples on pinching<br>- Pink to light brown (white skin dark brown to black (dark skin)<br>- Sometimes painful, tender, itchy<br>- 0.5–1.5 cm diameter |
| Melanocytic nevus | - Benign skin lesion due to a local proliferation of pigment cells<br>- Bepends on genetic factors, on sun exposure | - Any part of the body<br>- Flat or protruding<br>- Pink or flesh tones to dark brown steel blue, or black<br>- A few mm-cm in diameter |
| Vascular lesion | - Abnormalities of the skin and underlying tissues | - Infants and children and underlying tissues<br>- Tumors and malformations<br>- Red or purple<br>- Solid structure, called a red lump or lacune |

### 3.2 Transfer Learning with MobileNet

MobileNet's [5] integrated neural network has pre-trained over 1,280,000 images containing 1,000 object layers from the 2014 ImageNet challenge. The weights and features of the MobileNet model are pre-trained in the source domain ImageNet dataset. Then, they are transferred to the target domain for skin lesion classification.

The MobileNet architecture was adapted to classify skin images by replacing the last layer with a new fully connected, SoftMax, and classification output layer. The size of the output fully connected layer is $N \times 2048$, where N refers to the class number. Softmax is a common learning algorithm for multiple linear

classification functions. The softmax value for output $z_j$ is calculated by the Eq. 1:

$$\sigma(z_j) = \frac{e^{z_j}}{\sum_{k=1}^{K} e^{z_k}} \tag{1}$$

where $\sigma(z_j)$ is the softmax value, $z$ is a vector of inputs to the output layer and $j$ indexes the output units from 1, 2, 3, ..., K.

We use the MobileNet model for the following advantages: MobileNet is one of the most popular and widely used architectures because of its computational accuracy and performance. MobileNet has fewer parameters than some others, so it is easy to train. MobileNet applies depth-separated convolution, eliminating the dependence on depth when convolution. Using a pre-trained encoder helps the model converge faster than the untrained model.

### 3.3 Evaluation

The performance of the proposed model was evaluated using accuracy. Accuracy is the measure/indicator to evaluate the accuracy of the model by the ratio of the number of correctly detected skin images (with skin lesions and no skin lesions) to the total number of skin images, by the Eq. 2:

$$Accuracy = \frac{TP + TN}{TP + TN + FP + FN} \tag{2}$$

where: TP (True Positive): the number of skin images bearing the lesion label correctly classified into the lesion class. FP (False Positive): number of skin images bearing the non-lesion label correctly classified into the lesion class. FN (False Negative): number of skin images with lesion labels incorrectly classified into the non-lesional class. TN (True Negative): number of skin images bearing the non-lesion label correctly classified into the non-lesional class.

## 4 Processing

The skin lesion detection system model consists of three phases: Pre-processing, Segmentation, and Classification. Figure 2 shows the proposed system that is used in this research. We will describe experimental methods in each phase.

**Phase 1: Pre-processing:** The dataset contains images of skin lesions at different resolutions. However, the resolution of some high-resolution skin lesion images requires high computation costs. Therefore, it is necessary to resize the lesion image for the deep learning network.

Pre-processing of skin lesion images was performed by using the Keras[2] image_data_generator. Samples in the dataset have been scaled down to 224 ×

[2] https://keras.io/.

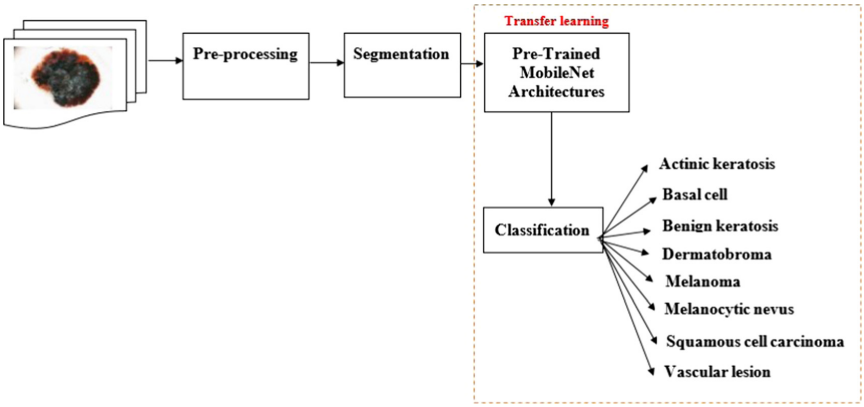


**Fig. 2.** Classification framework of skin lesions.

224 pixels from the different resolutions to make the images MobileNet compatible.

**Phase 2: Segmentation:** The segmentation must be efficient so that lesion information can be extracted with high confidence. Besides, the precision of this process directly affects the step of extraction characteristics. Therefore, an appropriate segmentation technique is crucial to obtain good classification results for the problem in question.

Image segmentation is the process of dividing an image into several segments (a set of pixels, also known as superpixels). The goal of image segmentation is to simplify the image for easy analysis. Image segments are often used to locate objects and boundaries. More precisely, image segmentation is a process of labeling every pixel in a sample so that pixels with the same label share fixed characteristics. The result of superpixels segmentation on a skin lesion image is shown in Fig. 3.

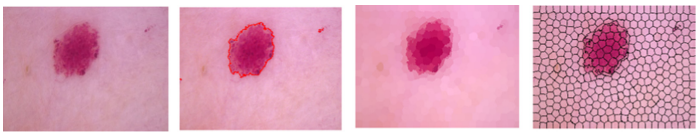

**Fig. 3.** Image segmentation based on Superpixels.

**Phase 3: Classification:** We classify the inlet test image into layers of skin lesions using the MobileNet model to reduce space and time to classify skin lesions. In image classification, the dataset is divided into training and testing on an 80:20 scale. The classification model is developed based on training templates using transfer learning. In the experiment, the accuracy of the learned model is

measured with the test dataset. We also use weights of the MobileNet network model trained on the ImageNet dataset. Dimensions of all images are determined by resizing to 224 × 224 for width, height. Table 2 shows the trainable and non-trainable parameters of the customized and fine-tuned models.

**Table 2.** Trainable and non-trainable parameters

| Model | Total parameters | Trainable |
|---|---|---|
| Customized Model | 2,268,232 | 10,248 |
| Fine Tuned Model | 2,268,232 | 2,257,984 |

## 5 Experiment

In our experiments, we identified three classification scenarios. In the first scenario, skin cancer classification, this study uses the image three categories: Melanoma, Basal cell carcinoma, and Squamous cell carcinoma. The second scenario, skin lesions classification, can classify the image into eight categories: Melanoma, Basal cell carcinoma, Squamous cell carcinoma, Actinic keratosis, Benign keratosis, Dermatofibroma, Melanocytic nevus, and Vascular lesion. In the third scenario, we change the learning rate.

In this section, Sect. 5.1 description the dataset. We present the tools used in Sect. 5.2. Section 5.3 presents the training and test dataset .We formulate scenarios to test the results and discussion in Sect. 5.4, Sect. 5.5, Sect. 5.6 and 5.7 respectively.

### 5.1 Dataset

International Skin Imaging Collaboration (ISIC) 2019[3] dataset provides 25,331 skin lesion images for training data shown in Table 3.

The ISIC 2019 dataset contains the HAM10000 [22] and BCN_20000 [23] and MSK [24]. HAM10000 contains 600 × 450 samples that are centered and cut around the lesion. This dataset is the older challenge of ISIC 2018. Whereas BCN_20000 contains samples of various sizes such as 600 × 450, 1024 × 671, 1024 × 679, 1024 × 680, 1024 × 682, 1024 × 685, 1024 × 764, 1024 × 768, 1024 × 1024, .... This dataset is difficult to classify because many samples have not been cropped, and lesions are in confusing and uncommon locations. Finally, the MSK dataset contains images of various sizes. Skin samples that are color swatches in JPG format are divided into eight classes shown in Fig. 1.

[3] https://challenge.isic-archive.com/data.

**Table 3.** The number of samples for each class in the dataset

| Diagnostic | Acronym | Sample |
|---|---|---|
| Actinic keratosis | AK | 867 |
| Basal cell carcinoma | BCC | 3,323 |
| Benign keratosis | BKL | 2,624 |
| Dermatofibroma | DF | 239 |
| Melanocytic nevus | NV | 12,875 |
| Melanoma | MEL | 4522 |
| Squamous cell carcinoma | SCC | 628 |
| Vascular lesion | VASC | 253 |

### 5.2 Tools

Our method has been deployed on an R [25] platform together with the tfhub, Keras library packages. RStudio is a free and open-source integrated development environment (IDE) for R. Using the tfhub library package provides R wrappers for the Tensorflow Hub. Tensorflow Hub is a library for reusable machine learning modules. Modules are an independent part of the Tensorflow Hub diagram and, together with weights, can be reused for different tasks in a process known as transfer learning.

### 5.3 Training and Test

The dataset is divided into two parts: 80% equivalent to 20,265 images for training and 20% with 5,066 images for test dataset shown in Table 4.

**Table 4.** The table describes the number of images per class of the training and test dataset.

| Diagnostic | Training | Test |
|---|---|---|
| Actinic keratosis | 694 | 173 |
| Basal cell carcinoma | 2,658 | 665 |
| Benign keratosis | 2,099 | 525 |
| Dermatofibroma | 191 | 48 |
| Melanocytic nevus | 10,300 | 2,575 |
| Melanoma | 3,618 | 904 |
| Squamous cell carcinoma | 502 | 126 |
| Vascular lesion | 203 | 50 |

### 5.4 Scenario 1: Skin Cancer Classification (3 Classes)

The classification was conducted experimentally on three cancer layers: Melanoma, Basal cell carcinoma, and Squamous cell carcinoma with a training sample number of 6,778 and a test dataset of 1,695. The scenario helps to classify cancer group in the dataset.

The pre-trained MobileNet delivered learning with the modified softmax to accommodate the three classes of skin lesions. When the number of epoch = 5, the model reached an accuracy of 0.7177, then increased epoch = 10, the accuracy reached 0.8179. The results experiment in Scenario 1 are shown in Table 5.

**Table 5.** Table comparing the results of three classes.

| Results | Epoch = 5 | Epoch = 10 |
|---|---|---|
| Training | 0.8146 | 0.8589 |
| Testing | 0.7177 | 0.8179 |

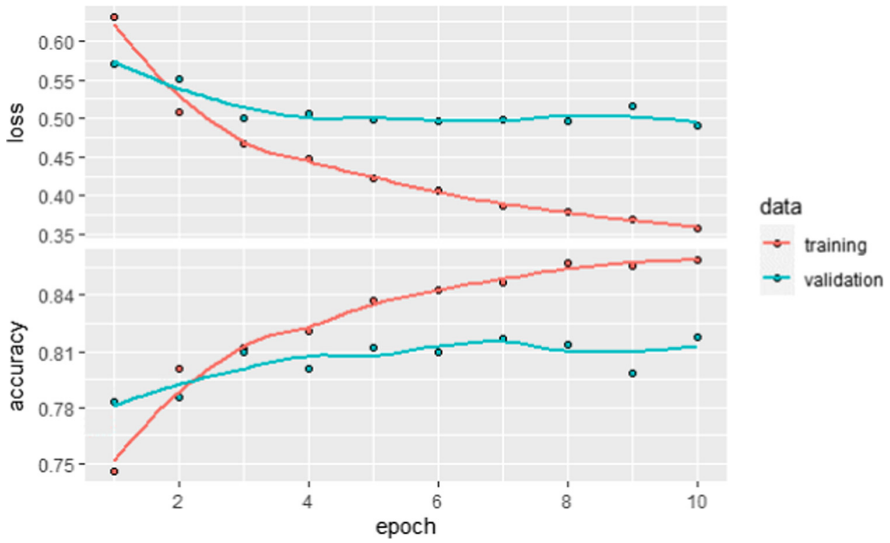


**Fig. 4.** Accuracy and loss with epoch = 10 (three-class classification).

Skin lesions classification performance in training and testing phases of the model for Scenario 1 with epoch = 10 shown in Fig. 4. Accuracy increases with the number of iterations along with the symmetrical downward slope of the loss curve. The average precision for ten runs is calculated as the overall accuracy of the model. The training loss is 0.358. The validation loss is 0.489.

### 5.5 Scenario 2: Skin Lesions Classification (8 Classes)

The second scenario can classify the image into eight categories: Melanoma, Basal cell carcinoma, Squamous cell carcinoma, Actinic keratosis, Benign keratosis, Dermatofibroma, Melanocytic nevus, and Vascular lesion. Similar to the three-tier classification, transfer learning is applied to pre-trained MobileNet, where the softmax is modified to work with eight classes. The number of epochs is trained 10, 20, and 40, respectively.

**Table 6.** Table comparing the results of eight classes.

| Results | Epoch = 10 | Epoch = 20 | Epoch = 40 |
|---|---|---|---|
| Training | 0.7361 | 0.7583 | 0.7679 |
| Testing | 0.6426 | 0.6604 | 0.6626 |

We conducted the classification on eight data classes with epoch = 10. The results achieved the accuracy on the Test set is 0.6426. Then, we increase the number of epochs = 20, the performance on the test set increases to 0.6604. Finally, the third experiment was performed with epoch number = 40. Table 6 gives an overview of the grading experiments' obtained results on eight layers. As the epoch number increases, the model's accuracy improves.

### 5.6 Scenario 3: Changing Learning Rate

This scenario is designed to compare the effect of changing the learning rate in the classification problem. First, we conduct experiments on three classes: Melanoma, Basal cell carcinoma, and Squamous cell carcinoma with the same number of samples as Scenario 1 with epoch = 5. Then, experiment on eight classes with a dataset as Scenario 2 and number epoch = 10. The results experiment in Scenario 3 are shown in Table 7.

**Table 7.** The table compares the effects of changing the learning rate.

| Results | Epoch = 5 | Epoch = 10 |
|---|---|---|
| Scenario 1 | 0.7177 | |
| Scenario 2 | | 0.6426 |
| Scenario 3 | 0.8011 | 0.6737 |

Table 7 shows the same training model. Again, when we change the learning rate to 0.0001, the classification results increase.

A comparative study was done with the ISIC 2019 rankings. In [26], the authors explore multi-resolution EfficientNets for skin lesion classification, combined with extensive data augmentation, loss balancing, and ensembling, achieving an accuracy rate of 63%. Our proposed method with accuracy is 66%. Furthermore, the accuracy of the proposed method increased when we changed the learning rate.

### 5.7 Discussion

The efficiency of transfer learning in multilayered CNN architecture with the MobileNet model is verified on a total of 25,331 skin lesions images from the ISIC 2019[4] dataset.

From the experimental results, the classification results in the three classes are always higher than the classification results in the eight classes. When we increase the classes to classify, the complexity of the scenario also increases. The factors that make it difficult for the classification are the similarity of the skin lesions, the uneven distribution of data among classes. Several images in the dataset are considered too homogeneous, which affects the accuracy of the classification.

The use of MobileNet in the classification of skin lesions to assist physicians in medical imaging tasks has improved. However, classification systems often require much time in training and need the hardware to have a GPU graphics card.

## 6 Conclusion

Detecting skin lesions is an area of great interest due to its importance in skin cancer prevention and early diagnosis of skin diseases.

First, we learn the characteristics of different skin lesions types from the ISIC 2019 dataset. Second, we apply the fractionation technique basing on superpixels to generate the lesion segmentation on the skin images. Third, we grasp transfer learning techniques and perform transfer learning under three scenarios basing on the MobileNet network model to predict skin images. Experimental results show that using transfer learning technology can help us train multitier CNN networks with only a limited set of data and satisfactory results. For image classification problems with small training datasets, transfer learning is one of the first solutions to use. When we use transfer learning, depending on the dataset, we choose an appropriate approach.

With the achieved results, classifying skin lesions by transfer learning method is expected to support doctors in diagnosing skin lesions, especially melanoma.

[4] https://challenge.isic-archive.com/data.

## References


1. Song, Y., et al.: Large margin local estimate with applications to medical image classification. IEEE Trans. Med. Imaging **34**(6), 1362–1377 (2015). https://doi.org/10.1109/tmi.2015.2393954
2. Albahar, M.A.: Skin lesion classification using convolution neural network with novel regularizer. IEEE Access **7**, 38306–38313 (2019). https://doi.org/10.1109/access.2019.2906241
3. Mahbod, A., Schaefer, G., Wang, C., Ecker, R., Ellinge, I.: Skin lesion classification using hybrid deep neural networks. In: IEEE International Conference on Acoustics, Speech and Signal Processing (ICASSP) (2019). https://doi.org/10.1109/icassp.2019.8683352
4. Pan, S.J., Yang, Q.: A survey on transfer learning. IEEE Trans. Knowl. Data Eng. **22**(10), 1345–1359 (2010). https://doi.org/10.1109/tkde.2009.191
5. Howard, A.G., et al.: MobileNets: efficient convolutional neural networks for mobile vision applications (2017). http://arxiv.org/abs/1704.04861
6. Deng, J., Dong, W., Socher, R., Li, L.-J., Li, K., Fei-Fei, L.: ImageNet: a large-scale hierarchical image database. In: IEEE Conference on Computer Vision and Pattern Recognition (2009). https://doi.org/10.1109/cvpr.2009.5206848
7. Sumithra, R., Suhil, M., Guru, D.S.: Segmentation and classification of skin lesions for disease diagnosis. Proc. Comput. Sci. **45**, 76–85 (2015). https://doi.org/10.1016/j.procs.2015.03.090
8. Akay, B.N., Kocyigit, P., Heper, A.O., Erdem, C.: Dermatoscopy of flat pigmented facial lesions: diagnostic challenge between pigmented actinic keratosis and lentigo maligna. Br. J. Dermatol. **163**(6), 1212–1217 (2010). https://doi.org/10.1111/j.1365-2133.2010.10025.x
9. Cameron, A., Rosendahl, C., Tschandl, P., Riedl, E., Kittler, H.: Dermatoscopy of pigmented Bowen's disease. J. Am. Acad. Dermatol. **62**(4), 597–604 (2010). https://doi.org/10.1016/j.jaad.2009.06.008
10. Lallas, A., et al.: The dermatoscopic universe of basal cell carcinoma. Dermatol. Pract. Conceptual **4**(3), 11–24 (2014). https://doi.org/10.5826/dpc.0403a02
11. Zaballos, P., et al.: Studying regression of seborrheic keratosis in lichenoid keratosis with sequential dermoscopy imaging. Dermatology **220**(2), 103–109 (2010)
12. Moscarella, E., et al.: Lichenoid keratosis-like melanomas. J. Eur. Acad. Dermatol. Venereol. **65**(3), e85–e87 (2011)
13. Braun, R.P., et al.: Dermoscopy of pigmented seborrheic keratosis: a morphological study. Arch. Dermatol. **138**(12), 1556–1560 (2002)
14. Zaballos, P., Puig, S., Llambrich, A., Malvehy, J.: Dermoscopy of dermatofibromas. Arch. Dermatol. **144**(1), 75–83 (2008). https://doi.org/10.1001/archdermatol.2007.8
15. Tschandl, P., Rosendahl, C., Kittler, H.: Dermatoscopy of flat pigmented facial lesions. J. Eur. Acad. Dermatol. Venereol. **29**(1), 120–127 (2014). https://doi.org/10.1111/jdv.12483
16. Schiffner, R., et al.: Improvement of early recognition of lentigo maligna using dermatoscopy. J. Am. Acad. Dermatol. **42**(1), 25–32 (2000). https://doi.org/10.1016/s0190-9622(00)90005-7
17. Rosendahl, C., Cameron, A., McColl, I., Wilkinson, D.: Dermatoscopy in routine practice - 'chaos and clues'. Aust. Fam. Phys. **41**(7), 482–487 (2012)
18. Zaballos, P., et al.: Dermoscopy of solitary angiokeratomas. Arch. Dermatol. **143**(3), 318–325 (2007). https://doi.org/10.1001/archderm.143.3.318

19. Zaballos, P., et al.: Dermoscopy of pyogenic granuloma: a morphological study. Br. J. Dermatol. **163**(6), 1229–1237 (2010). https://doi.org/10.1111/j.1365-2133.2010.10040.x
20. Stutz, D., Hermans, A., Leibe, B.: Superpixels: an evaluation of the state-of-the-art. Comput. Vis. Image Underst. **166**, 1–27 (2018). https://doi.org/10.1016/j.cviu.2017.03.007
21. Ren, X., Malik, J.: Learning a classification model for segmentation. In: Proceedings Ninth IEEE International Conference on Computer Vision (2003). https://doi.org/10.1109/iccv.2003.1238308
22. Tschandl, P., Rosendahl, C., Kittler, H.: The HAM10000 dataset, a large collection of multi-source dermatoscopic images of common pigmented skin lesions. Sci. Data **5**, 180161 (2018). https://doi.org/10.1038/sdata.2018.161
23. Combalia, M., et al.: BCN20000: dermoscopic lesions in the wild (2019). arXiv:1908.02288
24. Codella, N.C.F., et al.: Skin lesion analysis toward melanoma detection: a challenge at the 2017 international symposium on biomedical imaging (ISBI), hosted by the international skin imaging collaboration (ISIC) (2017). arXiv:1710.05006
25. Ihaka, R., Gentleman, R.: R: a language for data analysis and graphics. J. Comput. Graph. Stat. **5**(3), 299–314 (1996). https://doi.org/10.2307/1390807
26. Gessert, N., Nielsen, M., Shaikh, M., Werner, R., Schlaefer, A.: Skin lesion classification using ensembles of multi-resolution EfficientNets with meta data. MethodsX 100864 (2020). https://doi.org/10.1016/j.mex.2020.100864